




Article

Design of a Modified Compact Coupler with Unwanted Harmonics Suppression for L-Band Applications

Saeed Roshani ¹, Salah I. Yahya ^{2,3}, Sobhan Roshani ^{1,*}, Amir Hossein Farahmand ¹ and Siroos Hemmati ⁴

- ¹ Department of Electrical Engineering, Kermanshah Branch, Islamic Azad University, Kermanshah 1477893855, Iran; s_roshany@yahoo.com (S.R.); amhofarahmand@gmail.com (A.H.F.)
- ² Department of Communication and Computer Engineering, Cihan University-Erbil, Erbil 44001, Iraq; salah.yahya@cihanuniversity.edu.iq or salah.ismaeel@koyauniversity.org
- ³ Department of Software Engineering, Faculty of Engineering, Koya University, Koya KOY45, Iraq
- ⁴ Department of Electrical Engineering, Faculty of Energy, Kermanshah University of Technology, Kermanshah 6715685420, Iran; s.hemmati@kut.ac.ir
- * Correspondence: sobhan_roshany@yahoo.ca

Abstract: This paper presents the design, analysis, and fabrication of a new miniaturized microstrip branch line coupler (BLC) with high harmonics suppression. The T-shaped resonators, open stubs cross-shaped resonators and radial stubs are used in the proposed coupler design. The designed BLC operates at 1 GHz frequency, which can suppress up to 5th spurious harmonics with a 20 dB level of attenuation. High miniaturization of about 86% is obtained for the proposed BLC, which is corresponding to the normalized size of $0.009 \lambda g^2$. The measured values of isolation and return loss are obtained 28 dB and 29 dB, respectively, while the measured insertion loss of better than 0.2 dB is achieved at the operating frequency. Additionally, the operating bandwidth of the designed coupler ranges from 0.905 GHz up to 1.105 GHz, which shows a 200 MHz operating bandwidth or a fractional bandwidth (FBW) of 20%. The presented BLC is fabricated and measured, where the measurements confirm the simulated results. The designed coupler shows desirable performance compared to the recent designed couplers.

Keywords: branch line coupler (BLC); fractional bandwidth; harmonic suppression; resonators; size reduction



Citation: Roshani, S.; Yahya, S.I.; Roshani, S.; Farahmand, A.H.; Hemmati, S. Design of a Modified Compact Coupler with Unwanted Harmonics Suppression for L-Band Applications. *Electronics* **2022**, *11*, 1747. <https://doi.org/10.3390/electronics11111747>

Academic Editors: Mohammad Maktoomi, Tutku Karacolak, Mohamed Helaoui and Syed Azeemuddin

Received: 21 April 2022

Accepted: 30 May 2022

Published: 31 May 2022

Publisher's Note: MDPI stays neutral with regard to jurisdictional claims in published maps and institutional affiliations.



Copyright: © 2022 by the authors. Licensee MDPI, Basel, Switzerland. This article is an open access article distributed under the terms and conditions of the Creative Commons Attribution (CC BY) license (<https://creativecommons.org/licenses/by/4.0/>).

1. Introduction

Millimeter and microwave wave communications are pioneer solutions for the high traffic processing of data in the next generations of the communication systems [1]. The couplers are widespread devices in the microwave and RF frequency applications [2]. Among the couplers, which have several types, branch line couplers (BLCs) are more prevalent. The couplers are important devices in balanced power amplifier [3,4], balanced mixer [5] and Doherty power amplifier [6] applications. The couplers can also be used for power division in many applications [7].

A common technique to provide size reduction and harmonic suppression is using stepped impedances [8] and open subs [9,10], which also have been used in the coupler structure [11–17]. A BLC using discontinuous microstrip lines is presented in [11], which obtained 60% size reduction. However, this BLC cannot suppress the unwanted harmonics. A BLC using quasi-lumped and T-shaped structures is presented in [12]. This BLC is designed to be nonsymmetrical, which shows 70% size reduction, but it cannot suppress the unwanted harmonics. Another compact BLC is presented in [13] using resonant cells, which achieved 80% size reduction. This BLC can suppress 3rd up to 7th harmonics. In [14], a BLC using stepped impedances is presented, which obtained 50% size reduction, but it has no harmonic suppression. A BLC with harmonics suppression is described in [15]. High impedance lines and internal shunt capacitors are used in this structure. The BLC

in [15] shows about 74% size reduction, but it has a large insertion loss of about 1 dB and only 2nd harmonic suppression. A squared coupler is presented in [16], which can suppress only 2nd harmonic using the slow wave technique. In [17], a wide band three sections BLC is presented. High size reduction was achieved in this coupler; however, only the 2nd harmonic is suppressed in this work.

Using open stubs in the main branches of the coupler is a technique which has been widely used for harmonic suppression and size reduction [18–24]. In this technique, squared or radial open stubs can be used in each main quarter wavelength lines. These open stubs can produce transmission zeros and provide wide stopband for the coupler. Additionally, the applied open stubs reduce the overall size of the coupler.

The presented coupler in [18] can suppress up to 5th harmonics, but it is not very compact. Another H-shaped resonator coupler is designed in [19]. The applied H-shaped resonators result in 64% size reduction, but the obtained stopband is not very wide. A coupler with T-shaped resonators is presented in [20]. This coupler has harmonic suppression up to 8th harmonics and good size reduction. However, the insertion loss of the coupler is not acceptable. Radial stubs are used to design a coupler in [21], which resulted in harmonics suppression and acceptable size reduction, but the second harmonic is not well attenuated. In [22], a compact microstrip coupler with good harmonic suppression is introduced using eight open-ended stubs, placed inside the coupler structure, which effectively reduces the circuit size about 80%. This structure works at 0.96 GHz and suppresses 2nd to 6th harmonics, but this device has complex structure and high insertion loss (0.3 dB). In [23], a microstrip coupler is designed at 1 GHz, using spiral open stubs, which resulted in 63% size reduction. This device only suppresses 2nd and 3rd harmonics and has high insertion loss (0.3 dB), which is undesirable. In [24], a miniaturized coupler at 2.1 GHz is designed with 63% size reduction using the spiral T-shaped transmission line. This device only suppresses 2nd and 3rd harmonics and has high insertion loss (0.9 dB), which is not acceptable.

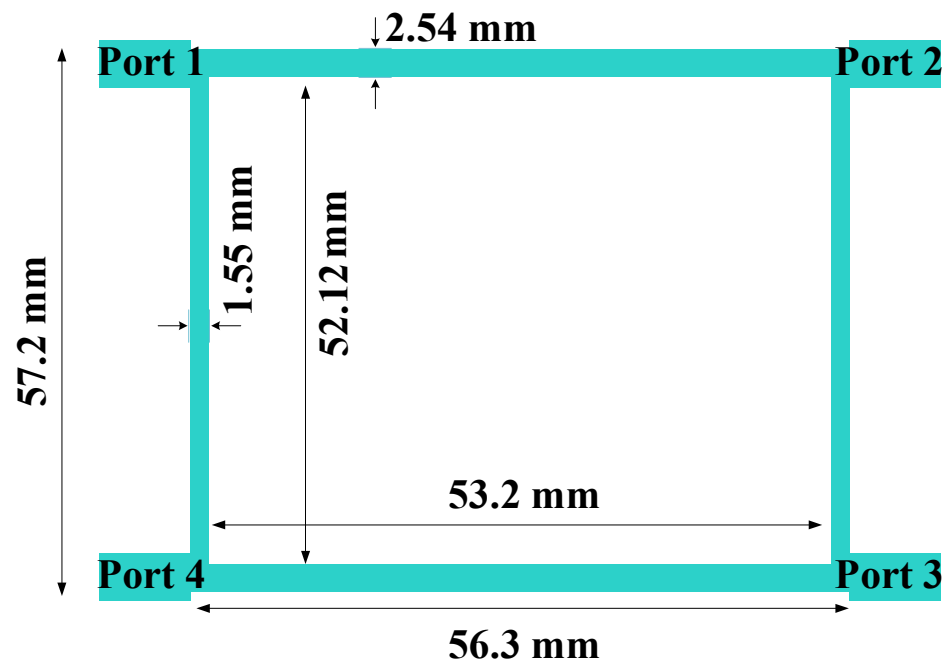
In the coupler design, dimensions of the applied lines have a direct effect on the coupler performance. In order to find the best performance, the length and width of the applied stubs should be obtained. To realize the best dimensions of the stubs, neural networks and artificial intelligence can be used [25,26]. In [27], a neural network design approach is presented for filters and resonators, which can be used for microwave couplers. In [28], a compact band pass filter with 7th-order harmonics suppression is proposed, which has a compact size and provides a wide rejection band. This filter can be used easily in the coupler structure.

In this paper, the proposed BLC is designed, simulated and measured. The fabrication is realized on a RT-Duroid substrate with a thickness of 0.508 mm and dielectric constant of 2.2. Several different resonators are exploited to design the presented BLC with high miniaturization and suppressing ability.

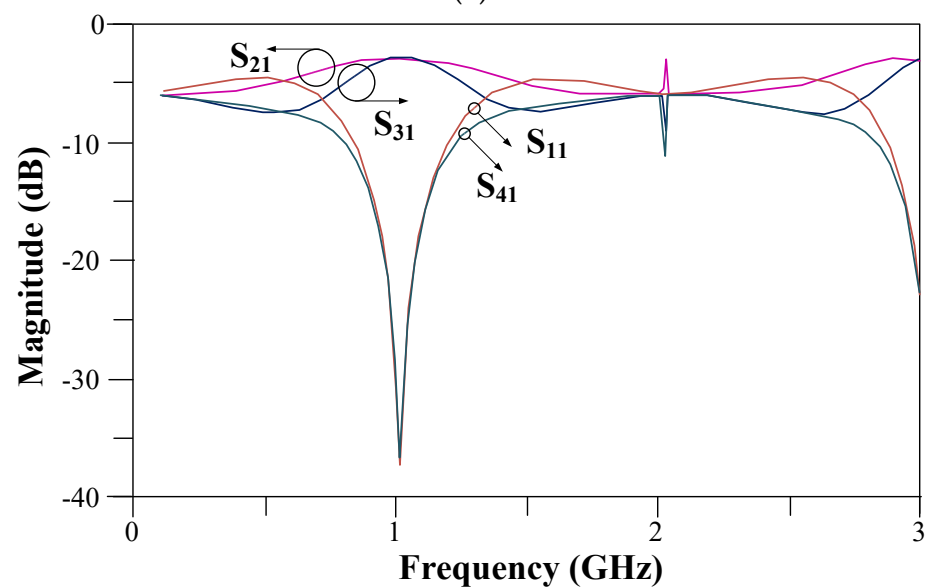
2. Design Procedure

This section explains how T-shaped stubs, radial stubs, cross-shaped resonators and open-ended stubs can be used to create the proposed branch line coupler (BLC). At the first step, a conventional BLC is formed at the operating frequency of 1 GHz. The structure of a conventional coupler is shown in Figure 1a, and its frequency response is depicted in Figure 1b.

Design procedure of the proposed BLC is illustrated in Figure 2. In step 1, the circuit of the initial resonator is presented. In step 2, the presented circuit is analyzed, and the related equations are extracted. Then, the transmission zeros of the resonator can be tuned to form the desired frequency response. The horizontal and vertical resonators, realized from the initial resonator, are obtained as illustrated in steps 3.1 and 3.2. Finally, the horizontal and vertical branches of the typical couplers are replaced with the proposed horizontal and vertical resonators, respectively.



(a)



(b)

Figure 1. BLC operating at 1 GHz: (a) conventional structure and (b) frequency response. All dimensions are in the millimeter unit.

2.1. Horizontal Resonator Design

To add harmonics suppression in the designed coupler, several resonators should be added in the main conventional structure. At first, an initial horizontal resonator is presented to obtain initial suppression band. The LC equivalent circuit (LCEC) of the proposed initial horizontal resonator is shown in Figure 3. Additionally, the frequency response of the presented LC circuit is compared with the frequency response of the layout transmission line realization in Figure 4. The applied values of the LC components for the LCEC of the proposed initial horizontal resonator are listed in Table 1.

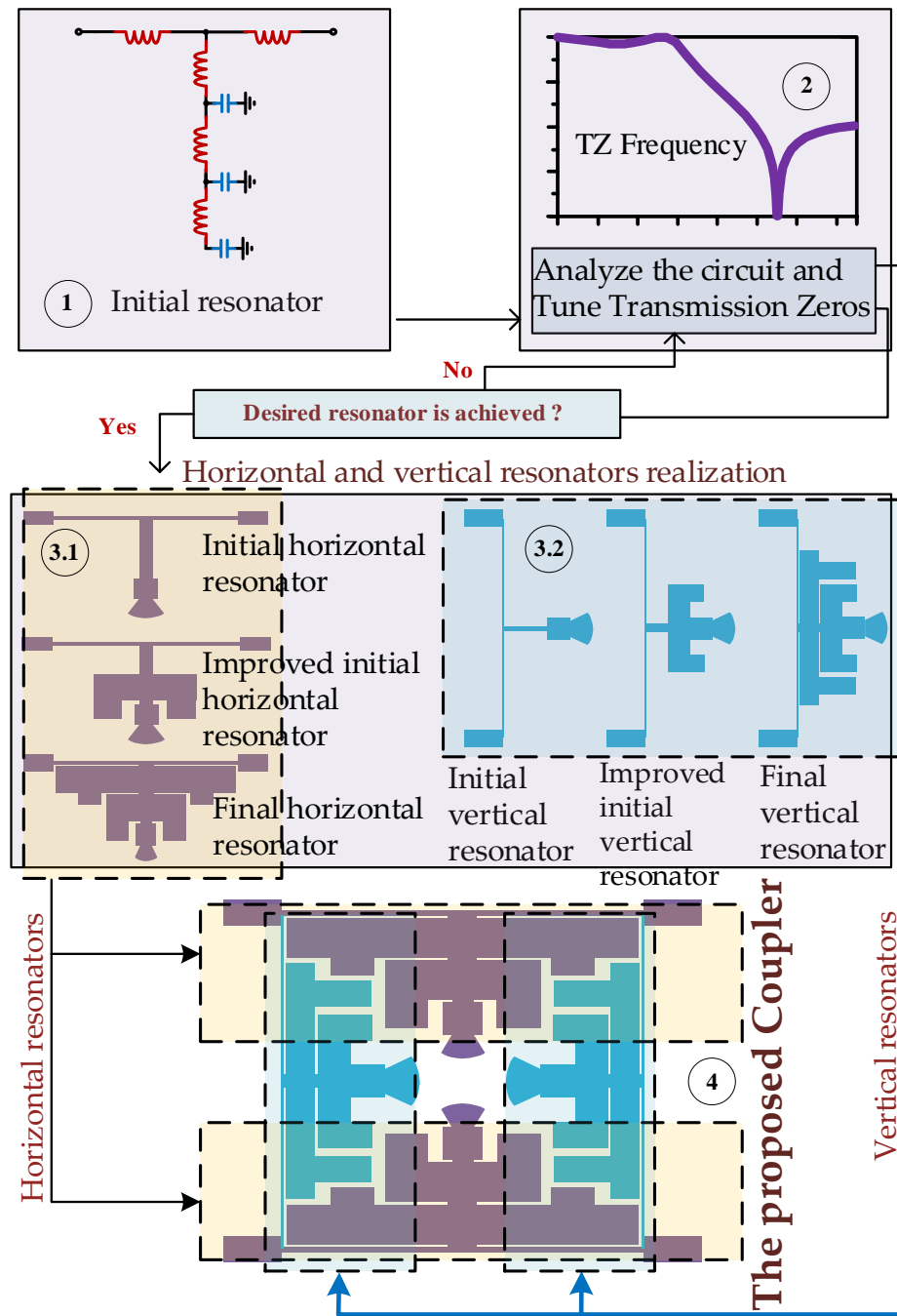


Figure 2. Design procedure of the proposed BLC.

Table 1. LC components values for the LCEC of the proposed initial horizontal.

LC Horizontal						
L_0	L_1	L_2	L_3	C_1	C_2	C_3
4.1 nH	0.6 nH	0.4 nH	0.3 nH	0.5 pF	0.4 pF	0.2 pF

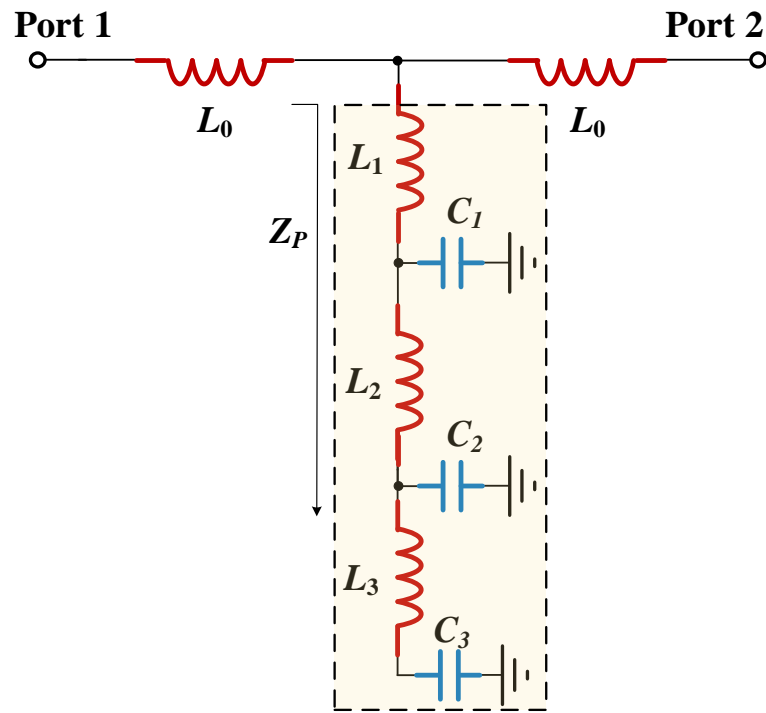


Figure 3. LCEC of the proposed initial horizontal resonator.

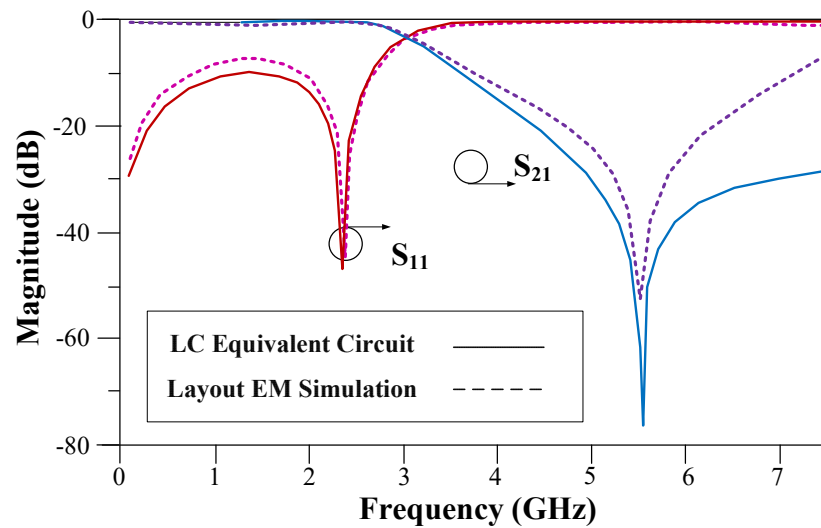


Figure 4. Frequency response of the presented LC circuit, as compared with the frequency response of the layout transmission line realization.

To determine the transmission zeros of the presented LCEC, the transfer function of the proposed initial horizontal resonator should be obtained. The extraction of the transfer function of the presented resonator is explained as follows. At first, the value of the Z_P impedance can be written as shown in (1).

$$Z_P = L_1 S + \frac{L_2 S + \frac{\frac{1}{C_3 S} + L_3 S}{C_2 S \left(\frac{1}{C_2 S} + \frac{1}{C_3 S} + L_3 S \right)}}{C_1 S \left(\frac{1}{C_1 S} + L_2 S + \frac{\frac{1}{C_3 S} + L_3 S}{C_2 S \left(\frac{1}{C_2 S} + \frac{1}{C_3 S} + L_3 S \right)} \right)} \quad (1)$$

By obtaining the value of Z_p , the transfer function of $H(S)$ can be calculated as written in (2).

$$H(S) = \frac{R Z_p}{\left(L_0 S + \frac{Z_p(R+L_0 S)}{R+Z_p+L_0 S}\right) (R + Z_p + L_0 S)} \tag{2}$$

where in (2), the parameter ‘ R ’ represents the 50Ω impedance of the port. The magnitude of the extracted transfer function, $H(S)$, is illustrated in Figure 5. As seen, the main transmission zero, which is extracted using analyses, equal to 5.5 GHz, is identical to the obtained one by circuit and EM simulations.

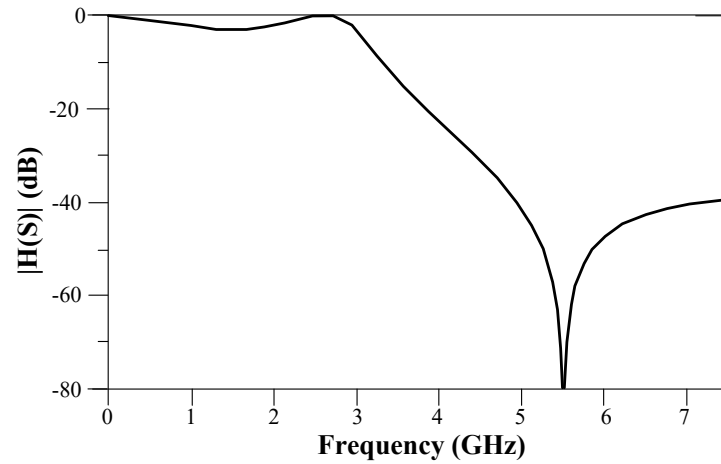


Figure 5. Magnitude of the extracted transfer function $H(S)$.

After obtaining the LCEC of the initial resonator, the microstrip transmission line realization can be achieved. The layout structure and frequency response of the initial horizontal resonator is depicted in Figure 6a,b.

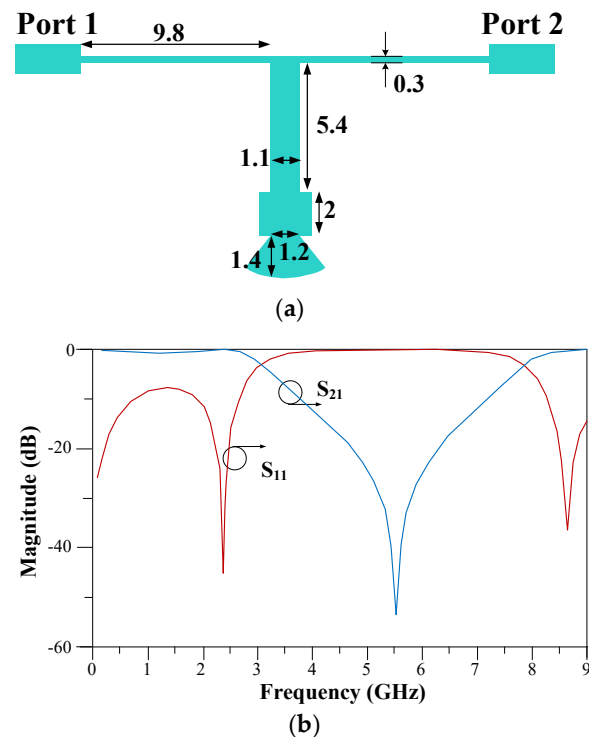


Figure 6. Initial horizontal resonator: (a) layout and (b) frequency response. All dimensions are in the millimeter unit.

As seen in Figure 6b, the frequency response of the initial horizontal resonator is not perfect in the passband and suppression band, so the initial horizontal resonator should be improved. The structure of the improved initial horizontal resonator and its frequency response are shown in Figure 7a,b.

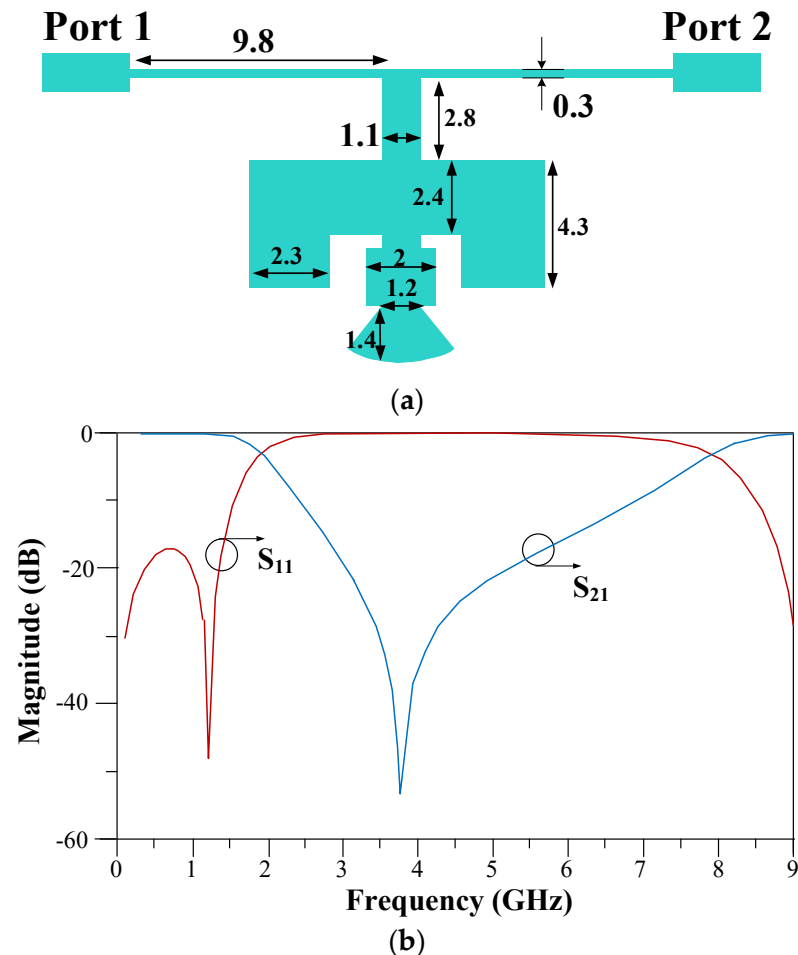


Figure 7. Improved initial horizontal resonator: (a) layout and (b) frequency response. All dimensions are in the millimeter unit.

To increase the suppression band and to modify the cut-off frequency, a stepped impedance resonator is added into the improved initial horizontal resonator structure, which forms the final horizontal resonator. The layout and frequency response of final horizontal resonator are shown in Figure 8a,b. As can be seen, the frequency response of the initial horizontal resonator is improved and optimized by adding the stepped impedance resonators in two steps, which finally have formed the final horizontal resonator. These added stepped impedance resonators in the first and second steps are shown by Resonator1 and Resonator2 in Figure 8. Resonator1 is added in the first step to form the improved initial horizontal resonator, and Resonator2 is added in the second step to form the final horizontal resonator. The stepped impedance resonators can create poles and zeros in the frequency response. The added poles improve the pass band, flatten the S_{21} parameter and decrease the return loss parameters. In addition, the added zeros widen the suppression band and improve the harmonic suppression ability of the resonator.

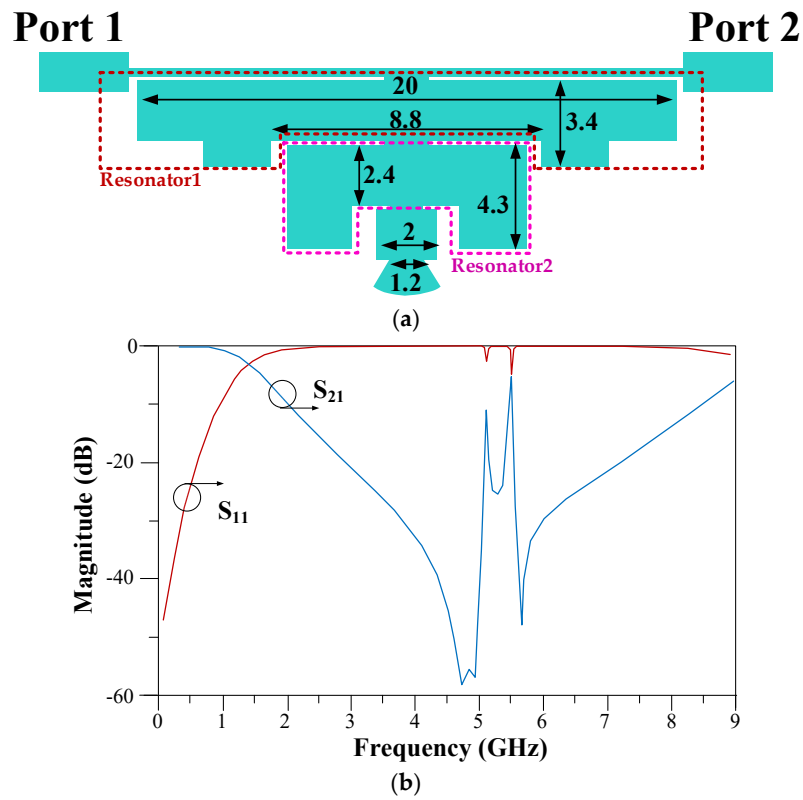


Figure 8. Final horizontal resonator: (a) layout and (b) frequency response. All dimensions are in the millimeter unit.

2.2. Vertical Resonator Design

The vertical resonators can be designed similar to horizontal resonators. The initial vertical resonator is designed based on the horizontal one. The layout and frequency responses of the initial vertical resonator are shown in Figure 9a,b.

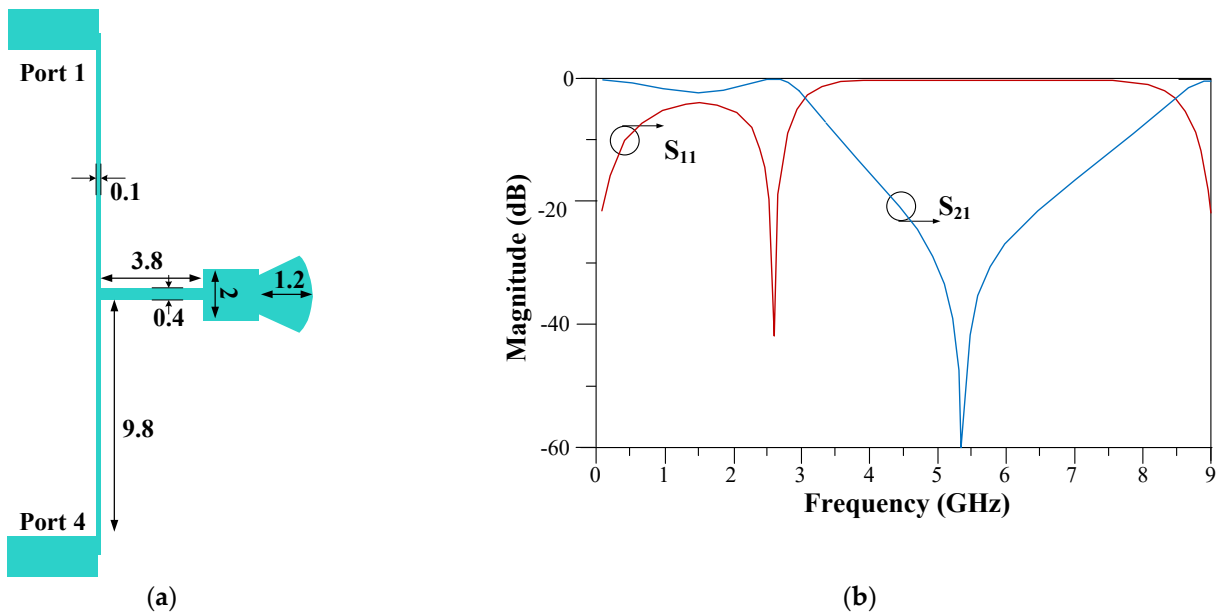


Figure 9. Initial vertical resonator: (a) layout and (b) frequency response. All dimensions are in the millimeter unit.

To improve the frequency response, the layout of initial vertical resonator is improved, which the improved initial vertical resonator is obtained by adding a stepped impedance resonator. The layout and frequency response of the improved initial vertical resonator is illustrated in Figure 10a,b.

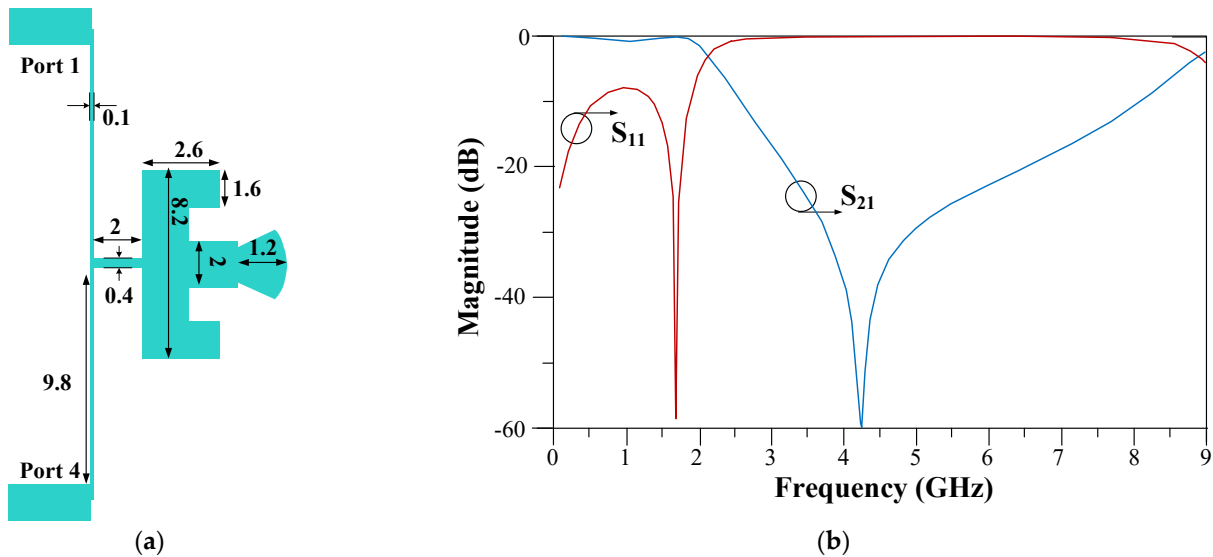


Figure 10. Improved initial vertical resonator: (a) layout and (b) frequency response. All dimensions are in the millimeter unit.

The final vertical resonator can be obtained by adding another stepped impedance resonator to the improved initial vertical resonator. The layout and frequency response of the final vertical resonator is shown in Figure 11.

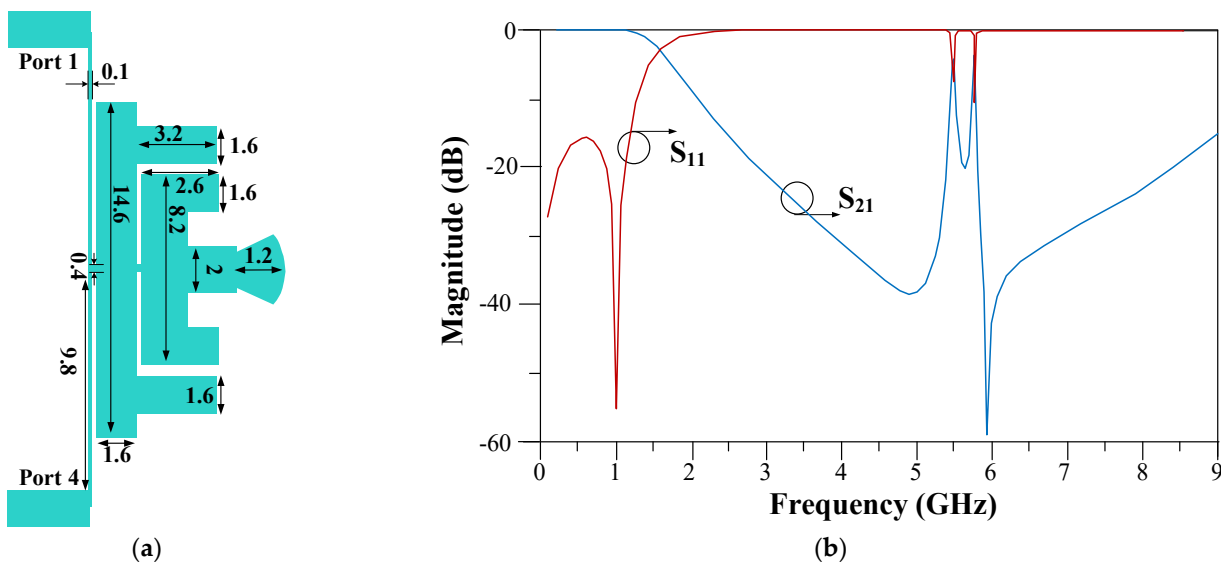


Figure 11. Final vertical resonator: (a) layout and (b) frequency response. All dimensions are in the millimeter unit.

3. Design of The Proposed BLC

The proposed BLC is designed at 1 GHz. In this design, the dimensions of the transmission lines and open stubs are modified to reach the desired performances. The structure of the proposed BLC is depicted in Figure 12. Size reduction of the proposed microstrip coupler is 86%, compared to the conventional BLC.

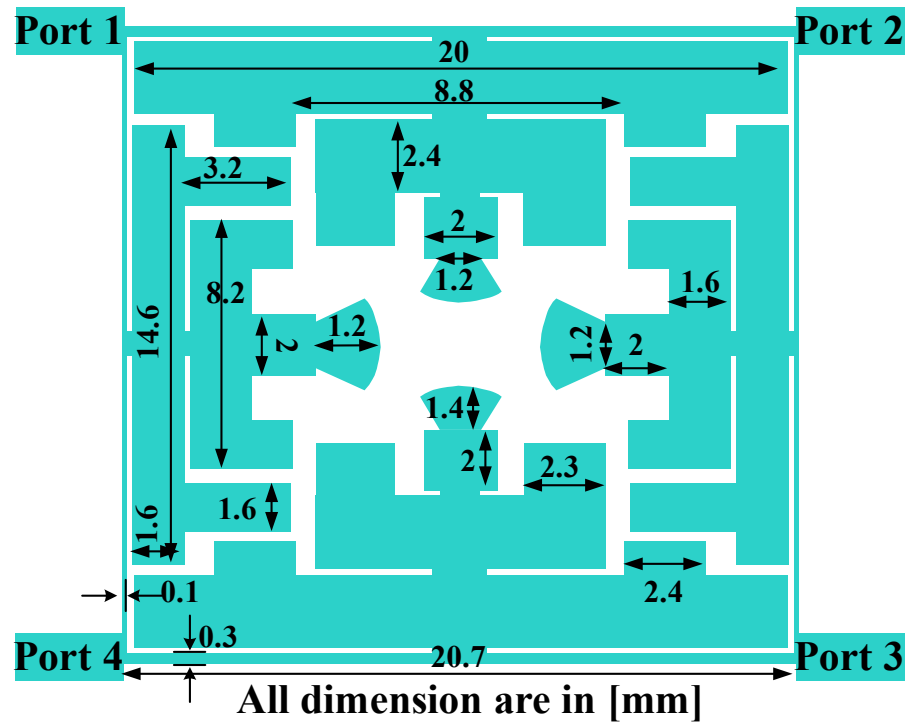


Figure 12. Structure of the proposed BLC.

The structures of the proposed and the conventional BLCs are compared in Figure 13. As seen, the proposed BLC only occupies 20.7 mm × 20.7 mm (0.093λ × 0.093λ), where the conventional one occupies 56.3 mm × 57.2 mm (0.25λ × 0.25λ). The proposed coupler only occupies less than 14% of the conventional coupler and shows more than 86% size reduction.

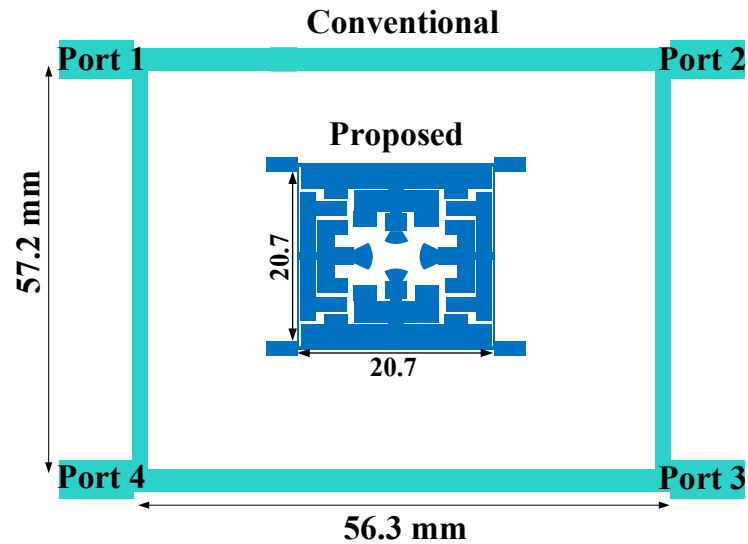


Figure 13. Structure of the proposed and the conventional BLCs.

Results of The Proposed BLC

The measured and simulated scattering parameters of the proposed BLC are depicted in Figures 14 and 15. The harmonics are attenuated in this design example with the respectively measured suppression levels of 15 dB, 21 dB, 28 dB, 35 dB, 32 dB, 25 dB, and 17 dB for the S_{21} parameter, while the corresponding attenuations are 26 dB, 43 dB, 44 dB, 35 dB, 50 dB, 55 dB, and 39 dB for the S_{31} parameter. Additionally, the obtained measured isolation and return loss are 28 dB and 29 dB, respectively.

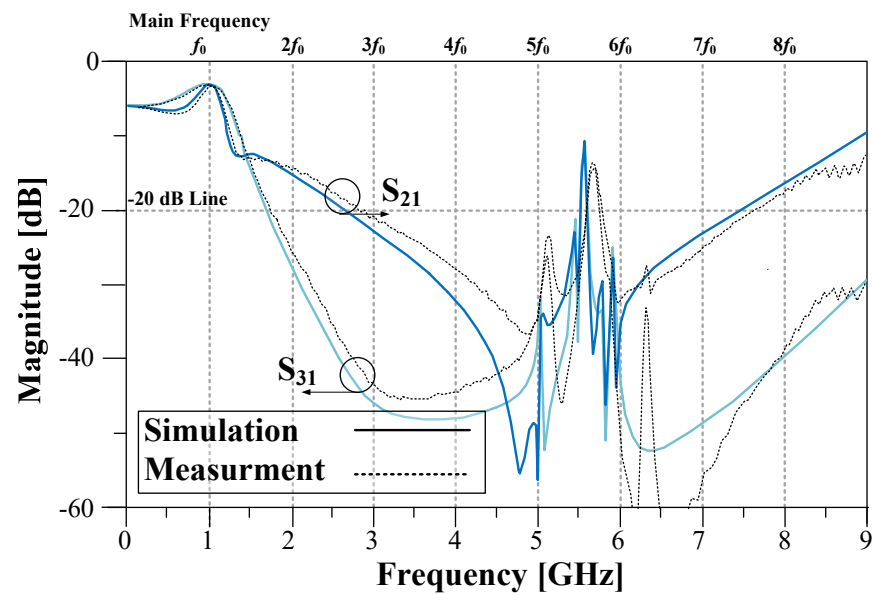


Figure 14. Measured and simulated S_{21} and S_{31} parameters of the proposed BLC.

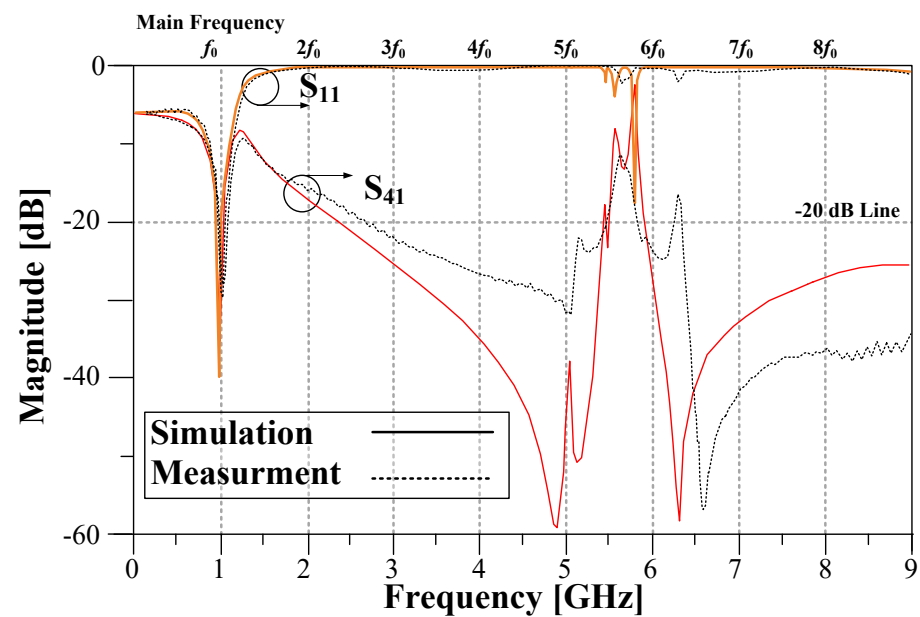


Figure 15. Measured and simulated S_{11} and S_{41} parameters of the proposed BLC.

The EM simulation in Advance Design System (ADS) software with adaptive step used is performed for simulation and the Hewlett Packard 8720B network analyzer with a linear measurement process with 22 MHz steps is used for measurement. The measurement and simulations results have good agreement, and a slight difference between these curves is normal.

Additionally, to show the performance of the designed BLC near the operating frequency, the in-band frequency response is illustrated in Figure 16. As seen, the fractional bandwidth (FBW) of the designed coupler is from 0.905 GHz up to 1.105 GHz, which show a 200 MHz operating bandwidth or FBW of 20%. The magnitudes of S_{21} and S_{31} in the FBW are located in the upper -4 dB line. The results show that the measured insertion loss of better than 0.2 dB is achieved at operating frequency.

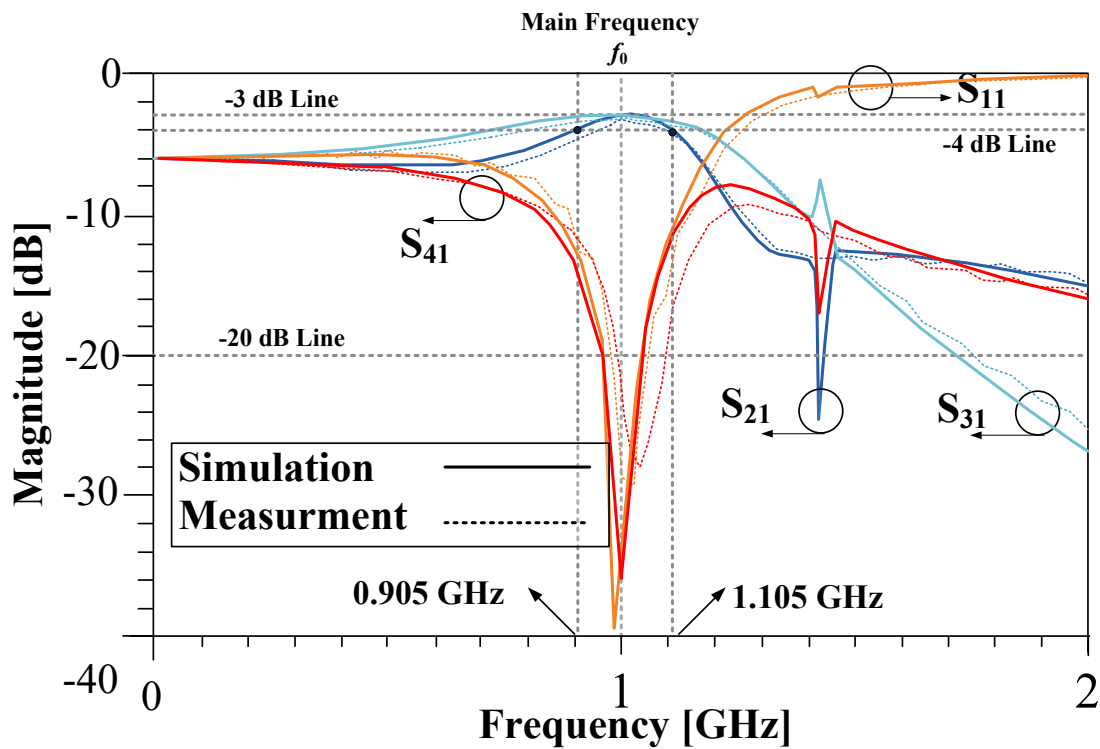


Figure 16. In-band simulated and measured S-parameters of the proposed BLC.

The result of the in-band phase difference is depicted in Figure 17. The measured phase difference of the presented BLC is less than $90 \pm 0.5^\circ$ at the main frequency. Moreover, the phase difference is flat, and its value is near 90° at the operating bandwidth.

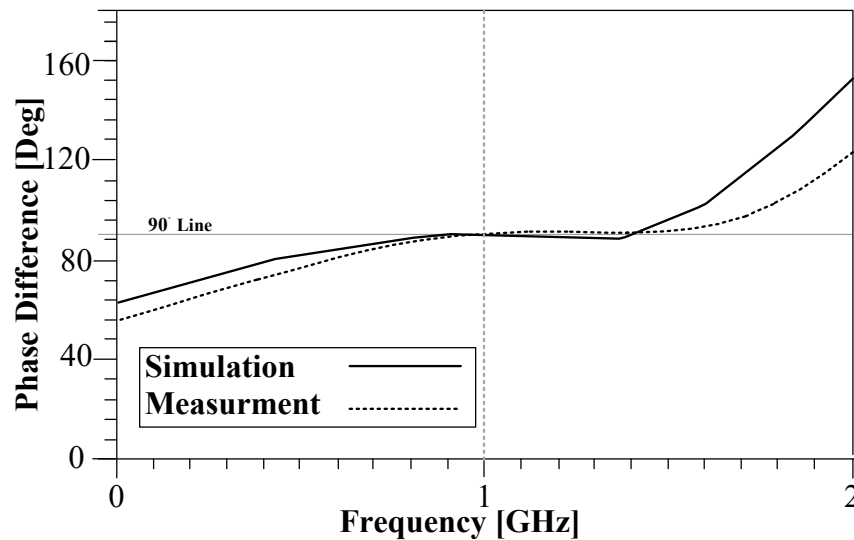


Figure 17. Measured and simulated phase difference in the proposed BLC.

The photos of the fabricated BLC under test are depicted in Figure 18. The Hewlett Packard 8720 B network analyzer is used to measure the fabricated device, the applied network analyzer has a linear measurement process with 22 MHz step.

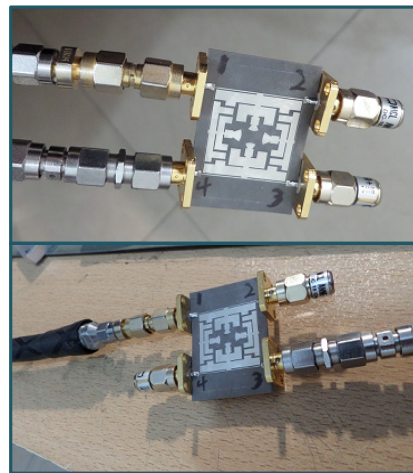


Figure 18. Photos of the fabricated BLC under test.

Table 2 shows the performance comparison between the proposed microstrip coupler and the recent ones. As can be seen from the table, the proposed BLC has the best performance in terms of insertion loss, harmonic suppression and size reduction between the cited research.

Table 2. Performance comparison between the proposed BLC and the recent ones.

Refs.	Frequency (GHz)	Insertion Loss (dB)	Harmonic Suppression	Size Reduction	Advantage	Technique
[11]	1	N/A	No	60%	Size reduction	Discontinuous microstrip lines
[12]	2.4	N/A	No	70%	Size Reduction	Quasi-lumped elements approach
[14]	1	0.33	No	50%	Size reduction	Step impedance transmission line
[15]	0.836	0.9	No	74%	Size reduction	Branch-line hybrid coupler
[16]	2	0.36	$2f_0$	72%	Size reduction Wideband	Slow wave
[18]	2.45	0.45	$2f_0$ to $5f_0$	55%	Harmonic suppression	L-shaped Open stubs
[19]	0.9	0.3	$2f_0$ to $4f_0$	64%	Size reduction Wideband	H-shaped microstrip line
[22]	0.96	0.3	$2f_0$ to $6f_0$	80%	Size reduction	Eight open ended stubs
[23]	1	0.3	$2f_0$ and $3f_0$	63%	Size reduction	Spiral open stubs
[24]	2.1	0.9	$2f_0$ and $3f_0$	63%	Size reduction	Spiral T-shaped lines
[29]	3.5 GHz	0.5	$2f_0$	No	Wideband Filtering	Coupled lines Open Stubs
[30]	3.5 GHz	0.5	No	35%	Size reduction	Pi-Network
[31]	0.9	0.76	No	36%	Size reduction Flexible	Open stub Meander lines
This work	1	0.2	$2f_0$ to $5f_0$	86%	Size reduction harmonic suppression	T-shaped resonators, Open stubs, Step impedance, and Radial stubs

4. Conclusions

A new BLC is designed, simulated and fabricated in this paper. The T-shaped resonators, open stubs, cross-shaped resonators, stepped impedance resonators, and radial stubs are used in the designed coupler. A design procedure for the proposed BLC is pro-

vided and explained. The proposed resonator is analyzed, and the related equations are extracted. The microstrip realization of the proposed resonators are provided, which are finally incorporated in the typical BLC structure to form the proposed coupler. The designed BLC is very compact and has the harmonics suppression ability. The simulated results are confirmed by the measured results. The results show more than 86% size reduction of the proposed device, compared with the conventional one, which make the proposed device suitable for modern communication systems applications. Finally, the performance of the designed coupler is compared with several state-of-the-art couplers, which show the advantages of the proposed coupler. In the future work, the design process of the proposed coupler will be improved with the help of artificial intelligence and deep learning methods.

Author Contributions: Conceptualization, S.R. (Sobhan Roshani), S.H. and S.R. (Saeed Roshani); methodology, S.R. (Sobhan Roshani), A.H.F. and S.R. (Saeed Roshani); software, A.H.F. and S.R. (Saeed Roshani); validation, S.I.Y.; formal analysis, S.I.Y., and S.R. (Saeed Roshani); investigation, S.R. (Saeed Roshani); resources, S.R. (Sobhan Roshani), and S.H.; writing—original draft preparation, S.I.Y. and S.R. (Saeed Roshani); writing—review and editing, S.R. (Sobhan Roshani), and S.I.Y.; visualization, S.R. (Saeed Roshani), and S.I.Y.; supervision, S.R. (Saeed Roshani); project administration, All authors have read and agreed to the published version of the manuscript.

Funding: This research received no external funding.

Data Availability Statement: All the material conducted in the study is mentioned in article.

Conflicts of Interest: The authors declare no conflict of interest.

References

1. Salh, A.; Audah, L.; Abdullah, Q.; Aydogdu, O.; Alhartomi, M.A.; Alsamhi, S.H.; Almalki, F.A.; Shah, N.S.M. Low Computational Complexity for Optimizing Energy Efficiency in mm-wave Hybrid Precoding System for 5G. *IEEE Access* **2021**, *10*, 4714–4727. [[CrossRef](#)]
2. Lalbakhsh, A.; Mohamadpour, G.; Roshani, S.; Ami, M.; Roshani, S.; Sayem, A.S.; Alibakhshikenari, M.; Koziel, S. Design of a Compact Planar Transmission Line for Miniaturized Rat-Race Coupler with Harmonics Suppression. *IEEE Access* **2021**, *9*, 129207–129217. [[CrossRef](#)]
3. Powell, J.R.; Sheppard, D.J.; Quaglia, R.; Cripps, S.C. A Power Reconfigurable High-Efficiency X-Band Power Amplifier MMIC Using the Load Modulated Balanced Amplifier Technique. *IEEE Microw. Wirel. Compon. Lett.* **2018**, *28*, 527–529. [[CrossRef](#)]
4. Kizilbey, O.; Palamutcuogullari, O.; Yarman, S.B. 3.5–3.8 GHz classE balanced GaNHEMT power amplifier with 20 W Pout and 80% PAE. *IEICE Electron.* **2013**, *10*, 20130104. [[CrossRef](#)]
5. Mohyuddin, W.; Kim, I.B.; Choi, H.C.; Kim, K.W. Design of A Compact Single-Balanced Mixer for UWB Applications. *J. Electromagn. Eng. Sci.* **2017**, *17*, 65–70. [[CrossRef](#)]
6. Zhang, Z.; Cheng, Z.; Liu, G. A Power Amplifier with Large High-Efficiency Range for 5G Communication. *Sensors* **2020**, *20*, 5581. [[CrossRef](#)] [[PubMed](#)]
7. Jamshidi, M.B.; Roshani, S.; Talla, J.; Roshani, S.; Peroutka, Z. Size reduction and performance improvement of a microstrip Wilkinson power divider using a hybrid design technique. *Sci. Rep.* **2021**, *11*, 7773. [[CrossRef](#)]
8. Lalbakhsh, A.; Alizadeh, S.M.; Ghaderi, A.; Golestanifar, A.; Mohamadzade, B.; Jamshidi, M.B.; Mandal, K.; Mohyuddin, W. A Design of a Dual Band Bandpass Filter Based on Modal Analysis for Modern Communication Systems. *Electronics* **2020**, *9*, 1770. [[CrossRef](#)]
9. Lalbakhsh, A.; Neyestanak, A.A.L.; Naser-Moghaddasi, M. Microstrip Hairpin Bandpass Filter Using Modified Minkowski Fractal for Suppression of Second Harmonic. *IEICE Trans. Electron.* **2012**, *95*, 78–81. [[CrossRef](#)]
10. Lalbakhsh, A.; Jamshidi, M.B.; Siahkamari, H.; Ghaderi, A.; Golestanifar, A.; Linhart, R.; Talla, J.; Simorangkir, R.B.V.B.; Mandal, K. A Compact Lowpass Filter for Satellite Communication Systems Based on Transfer Function Analysis. *AEU Int. J. Electron. Commun.* **2020**, *124*, 153318. [[CrossRef](#)]
11. Sun, K.O.; Ho, S.J.; Yen, C.C.; Van Der Weide, D. A compact branch line coupler using discontinuous microstrip lines. *IEEE Microw. Wirel. Compon. Lett.* **2005**, *15*, 519–520. [[CrossRef](#)]
12. Liao, S.S.; Pen, J.T. Compact planar microstrip branch line couplers using the quasi lumped elements approach with non-symmetrical and symmetrical T-shaped structure. *IEEE Trans. Microw. Theory Tech.* **2006**, *54*, 3508–3514. [[CrossRef](#)]
13. Kurgan, P.; Filipcewicz, J.; Kitlinski, M. Development of a compact microstrip resonant cell aimed at efficient microwave component size reduction. *IET Microw. Antennas Propag.* **2012**, *6*, 1291–1298. [[CrossRef](#)]
14. Sedighy, S.H.; Khalaj Amirhosseini, M. Compact branch line coupler using step impedance transmission lines (SITLs). *Appl. Comput. Electromagn. Soc. J.* **2013**, *28*, 866–870.

15. Tsai, K.-Y.; Yang, H.-S.; Chen, J.-H.; Chen, Y.-J. A Miniaturized 3 dB Branch-Line Hybrid Coupler with Harmonics Suppression. *IEEE Microw. Wirel. Compon. Lett.* **2011**, *21*, 537–539. [[CrossRef](#)]
16. Wang, J.; Wang, B.-Z.; Guo, Y.; Ong, L.C.; Xiao, S. A Compact Slow-Wave Microstrip Branch-Line Coupler with High Performance. *IEEE Microw. Wirel. Compon. Lett.* **2007**, *17*, 501–503. [[CrossRef](#)]
17. Barik, R.K.; Rajender, R.; Karthikeyan, S.S. A Miniaturized Wideband Three-Section Branch-Line Hybrid with Harmonic Suppression Using Coupled Line and Open-Ended Stubs. *IEEE Microw. Wirel. Compon. Lett.* **2017**, *27*, 1059–1061. [[CrossRef](#)]
18. Nie, W.; Xu, K.-D.; Zhou, M.; Xie, L.-B.; Yang, X.-L. Compact narrow/wide band branch-line couplers with improved upper-stopband. *AEU Int. J. Electron. Commun.* **2018**, *98*, 45–50. [[CrossRef](#)]
19. Krishna, I.S.; Barik, R.K.; Karthikeyan, S.; Kokil, P. A miniaturized harmonic suppressed 3 dB branch line coupler using H-shaped microstrip line. *Microw. Opt. Technol. Lett.* **2017**, *59*, 913–918. [[CrossRef](#)]
20. Kumar, K.V.; Karthikeyan, S.S. Miniaturised quadrature hybrid coupler using modified T-shaped transmission line for wide-range harmonic suppression. *IET Microw. Antennas Propag.* **2016**, *10*, 1522–1527. [[CrossRef](#)]
21. Hazeri, A.R.; Kashaninia, A.; Faraji, T.; Arani, M.F. Miniaturization and harmonic suppression of the branch-line coupler based on radial stubs. *IEICE Electron. Express* **2011**, *8*, 736–741. [[CrossRef](#)]
22. Lian, G.; Wang, Z.; He, Z.; Zhong, Z.; Sun, L.; Yu, M. A New Miniaturized Microstrip Branch-Line Coupler with Good Harmonic Suppression. *Prog. Electromagn. Res. Lett.* **2017**, *67*, 61–66. [[CrossRef](#)]
23. Kim, J.-S.; Kong, K.-B. Compact Branch-Line Coupler for Harmonic Suppression. *Prog. Electromagn. Res.* **2010**, *16*, 233–239. [[CrossRef](#)]
24. Choi, K.-S.; Yoon, K.-C.; Lee, J.-Y.; Lee, C.-K.; Kim, S.-C.; Kim, K.-B.; Lee, J.-C. Compact branch-line coupler with harmonics suppression using meander T-shaped line. *Microw. Opt. Technol. Lett.* **2014**, *56*, 1382–1384. [[CrossRef](#)]
25. Sattari, M.A.; Roshani, G.H.; Hanus, R.; Nazemi, E. Applicability of time-domain feature extraction methods and artificial intelligence in two-phase flow meters based on gamma-ray absorption technique. *Measurement* **2021**, *168*, 108474. [[CrossRef](#)]
26. Roshani, M.; Sattari, M.A.; Ali, P.J.M.; Roshani, G.H.; Nazemi, B.; Corniani, E.; Nazemi, E. Application of GMDH neural network technique to improve measuring precision of a simplified photon attenuation based two-phase flowmeter. *Flow Meas. Instrum.* **2020**, *75*, 101804. [[CrossRef](#)]
27. Jamshidi, M.B.; Lalbakhsh, A.; Mohamadzade, B.; Siahkamari, H.; Mousavi, S.M. A novel neural-based approach for design of microstrip filters. *AEU-Int. J. Electron. Commun.* **2019**, *110*, 152847. [[CrossRef](#)]
28. Luo, L.; Tie, H.; Ma, Q.; Zhou, B. Compact LTCC Filter with 7th-Order Harmonics Suppression for 5G N77 Band Applications. *Prog. Electromagn. Res. Lett.* **2021**, *98*, 69–74. [[CrossRef](#)]
29. Barik, R.K.; Koziel, S.; Szczepanski, S. Wideband Highly-Selective Bandpass Filtering Branch-Line Coupler. *IEEE Access* **2022**, *10*, 20832–20838. [[CrossRef](#)]
30. Maheswari, S.; Jayanthi, T. Design of Compact Branch-Line Coupler for Wi-Max Applications. *Int. J. Microw. Opt. Technol.* **2022**, *17*, 68–73.
31. Kumar, K.V.P.; Alazemi, A.J. A Flexible Miniaturized Wideband Branch-Line Coupler Using Shunt Open-Stubs and Meandering Technique. *IEEE Access* **2021**, *9*, 158241–158246. [[CrossRef](#)]